Taiwania, 59(3): 262–280, 2014
DOI: 10.6165/tai.2014.59.262

RESEARCH ARTICLE

Characterization and Expression Analysis of Stathmin Family Genes during Embryogenesis in Zebrafish, *Danio rerio*

De-Fen Shih[1,2#], Shian-Ling Chu[1#] and Shyh-Jye Lee[1,2,3,4,5*]

1. Institute of Zoology, National Taiwan University, 1 Roosevelt Rd., Section 4, Taipei, Taiwan 10617, R.O.C.
2. Department of Life Science, National Taiwan University, 1 Roosevelt Rd., Section 4, Taipei, Taiwan 10617, R.O.C.
3. Center for Biotechnology, National Taiwan University, 1 Roosevelt Rd., Section 4, Taipei, Taiwan 10617, R.O.C.
4. Research Center for Developmental Biology and Regenerative Medicine, National Taiwan University, 1 Roosevelt Rd., Section 4, Taipei, Taiwan 10617, R.O.C.
5. Center for Systems Biology, National Taiwan University, 1 Roosevelt Rd., Section 4, Taipei, Taiwan 10617, R.O.C.
** Corresponding author. Fax: 886-1-2-33662457; Tel.: 886-1-2-33665902; Email: jefflee@ntu.edu.tw*
[#] These two authors contribute equally.

(Manuscript received 07 Febuary 2014; accepted 04 April 2014)

ABSTRACT: Stathmin family genes are known to mediate microtubule disassembly that makes them potential regulators for integrating diverse intracellular signaling pathways. To investigate the roles of stathmins in zebrafish (*Danio rerio*) development, we cloned and characterized four zebrafish stathmin genes, including *stathmin 1b* (*stmn1b*), *stathmin-like 2a* (*stmn2a*), *stathmin-like 3* (*stmn3*), and *stathmin-like 4* (*stmn4*). All four stathmins contains a conserved stathmin-like domain with consensus phosphorylation domains and share high homology with their vertebral counterparts. RT-PCR and whole-mount *in situ* hybridization analyses revealed that zebrafish *stathmins* are mainly expressed in the central nervous system with divergent temporal and spatial expressions. This suggests roles of stathmins in neuronal regulation during development in zebrafish. By knocking down *stmn2a* we observed smaller brain, enlarge brain ventricle, brain edema and narrowed midbrain and hindbrain boundary. We also confirmed the observed phenotypes by using whole-mount ISH against *islet1* and found that *islet1* expression was reduced in *stmn2a* MO-injected embryos. In addition, these brain defects were specifically due to the loss of *stmn2a* because they could not be induced by a mis-match *stmn2a* MO and could be rescued by co-injecting *stmn2a* mRNA. Collectively, these results suggest a pivotal role of *stmn2a* in zebrafish brain development.

KEY WORDS: Embryogenesis, gene expression, stathmin, zebrafish.

INTRODUCTION

Microtubules mediate a variety of physiological processes such as mitotic spindle formation (Kline-Smith and Walczak, 2004) and axonal outgrowth (Bouquet and Nothias, 2007). They are highly dynamic by stochastically switching between growth and shortening states in a process called dynamic instability (Desai and Mitchison, 1997). Many proteins regulate microtubule dynamics, including stathmins, which are phosphoproteins known for their activity in regulating microtubule disassembly (Manna et al., 2006). The stathmin family genes, including stathmin, SCG10 (Anderson and Axel, 1985), SCLIP (Ozon et al., 1998), and RB3, with its splice variants RB3' and RB3" (Maucuer et al., 1993; Ozon et al., 1997; Ozon et al., 1998), are highly conserved among vertebrates, and serve as potential regulatory proteins integrating diverse intracellular signaling pathways (Koppel et al., 1990; Maucuer et al., 1993; Okazaki et al., 1993; Schubart et al., 1992; Sobel et al., 1989). Each member of stathmin family genes possesses a stathmin-like domain (SLD) with 65%~75% amino acid identities (Marklund et al., 1993; Schubart et al., 1989). The SLD is comprised of an N-terminal regulatory domain containing four phosphorylation sites and a C-terminal interaction domain possessing a predicted α-helical structure, which may potentially form a coiled-coil interaction with other proteins, such as KIS (an RNA-binding protein) (Maucuer et al., 1995), the Hsp70 chaperone (Manceau et al., 1999), and tubulin (Gigant et al., 2000; Redeker et al., 2000). With the exception of stathmin, SCG10, SCLIP, and RB3/RB3'/RB3", which are also called SCG10 family genes, contain an additional specific N-terminal extension composed of one to three domains. The conserved domain A of the N-terminal extension shares 57%~70% amino acid identities among SCG10 genes (Charbaut et al., 2005; Chauvin et al., 2008). In addition, two cysteine residues serve as palmitoylation sites (Lutjens et al., 2000; Stein et al., 1988), which may tether SCG10 proteins to Golgi membranes and other vesicle-like structures (Gavet et al., 2002). By contrast, the stathmin protein without the N-terminal extension is only found in the cytosol (Gavet et al., 1998; Koppel et al., 1990; Sobel et al., 1989).

Phosphorylation of stathmin is directed by numerous extracellular signals in various biological systems (Beretta et al., 1993; Chneiweiss et al., 1992; Doye et al., 1990; Leighton et al., 1993). Regulation through combinatorial phosphorylation leads stathmins toward appropriate biological responses by interacting with their respective targeting protein (Beretta et al., 1993; Curmi et al., 1994; Maucuer et al., 1990). Tubulin is the best characterized interacting partner for stathmin, as stathmins are known to modulate microtubule dynamics by sequestering free tubulins (Belmont et al., 1996; Charbaut et al., 2001; Grenningloh et al., 2004; Jourdain et al., 1997). It was also reported that extensive phosphorylation of stathmin occurs during mitosis (Brattsand et al., 1994; Luo et al., 1994; Strahler et al., 1992), which seems to be essential for progression of the cell cycle (Larsson et al., 1995; Lawler et al., 1998; Marklund et al., 1994). In mammals, the expression of stathmin is thought to be ubiquitous and neuron-enriched, whereas SCG10 family genes are mainly restricted in the nervous system (Ozon et al., 1999; Peschanski et al., 1993). SCG10, a well-known neural-specific phosphoprotein, was originally identified as a marker of neuronal differentiation (Anderson and Axel, 1985). The expressions of stathmin and SCG10 progressively increase during embryogenesis until birth and then decrease during postnatal development, but their regional expression domains in the brain greatly differ (Himi et al., 1994). SCLIP and RB3, members of the SCG10 family, are thought to be nervous system-specific. They are expressed during embryogenesis and persist into postnatal development and adulthood (Matsuo et al., 1998; Ozon et al., 1998). However, SCLIP has also been detected in non-neural tissues (Bieche et al., 2003). Altogether, each member of stathmin family genes has distinct regional and cellular localizations, suggesting that they diverged during neural evolution to acquire specific functions related to neuronal structural and functional plasticity.

Knockout of the stathmin gene in the mouse induced no major phenotype (Schubart et al., 1996) other than a mild late-onset axonopathy (Liedtke et al., 2002). The mild neuronal syndrome in stathmin-knockout mice might be due to the redundant and/or complementary effect of other family genes. For a more in-depth examination, stathmin was later found to be enriched in the amygdale, and stathmin-knockout mice showed defects in both learned and innate fear (Shumyatsky et al., 2005). In spite of the clear actions of stathmin family proteins on microtubule dynamics, which should influence many physiological functions, particularly neuronal regulation, their limited effects observed in mice studies prohibited us from fully characterizing their in vivo physiological roles in detail. Thus, an alternative animal model system is required to further investigate stathmin functions.

The zebrafish, *Danio rerio*, is an excellent model system for examining vertebrate development. The optical clarity of zebrafish embryos facilitates detailed microscopic analyses. Embryonic development proceeds rapidly after fertilization with the first cell division occurring within the first hour, and subsequent division proceeding at an increasingly rapid pace. Within 24 h, zebrafish possess a primary nervous system that is beginning to form functional connections.

In this study, we identified and cloned four stathmin genes: stathmin 1b (*stmn1b*), stathmin-like 2a (*stmn2a*), stathmin-like 3 (*stmn3*), and stathmin-like 4 (*stmn4*). Their sequences were analyzed and their expression patterns, particularly neuronal expression, were investigated. In addition, we show the loss of *stmn2a* induced brain defects in zebrafish embryos-injected with antisense morpholino (MO), implicating a critical role of *stmn2a* in brain development.

MATERIALS AND METHODS

Zebrafish maintenance, embryo production and culture

Wild-type zebrafish, *D. rerio*, were raised under a 14-h light/10-h dark cycle at 28.5°C. Eggs were collected at 15~20-min intervals after spawning, washed, and incubated in embryo medium (13.7 mM NaCl, 0.54 mM KCl, 0.025 mM Na_2HPO_4, 0.044 mM KH_2PO_4, 1.3 mM $CaCl_2$, 1.0 mM $MgSO_4$, and 0.42 mM $NaHCO_3$) at 28.5 °C until use. Embryos collected for whole-mount in situ hybridization were grown in embryo medium supplemented with 0.2 mM 1-phenyl-2-thiourea (Sigma, St. Louis, MO) to inhibit pigment formation. All animal handling procedures followed the guidelines for the use of laboratory animals at National Taiwan University, Taipei, Taiwan.

In silica cloning and sequence analysis

Candidate expressed sequence tags (ESTs) of zebrafish *stathmin* genes were identified by blasting human stathmin amino acid sequences (accession numbers listed in supplementary Table S1) against the NCBI zebrafish EST database. The zebrafish candidate orthologs of *stathmin 1*, *stathmin 2*, *stathmin 3,* and *stathmin 4* with a complete open reading frame were amplified by RT-PCR using primer pairs designed according to EST sequences or predicted sequences (Table S1). Deduced sequences of zebrafish stathmin family genes were aligned with putative orthologs from other species. Motif analyses of the four proteins were preformed using an online tool at the SMART website (http://smart.embl-heidelberg.de/). The amino acid sequences of zebrafish stathmins and orthologs of other

species were collected from NCBI (http://www.ncbi.nlm.nih.gov/) or Ensembl (http://www.ensembl.org/Danio_rerio/) websites; sequence alignments and phylogenetic analyses were performed using the MEGA4 software (Biodesign Institute, Tempe, AZ).

RT-PCR analysis

Total RNAs were prepared from adult tissues and early embryos using TRIzol reagent (Invitrogen). To synthesize single-stranded cDNA, 3 μg of total RNA, oligo dT primer, and M-MLV Reverse Transcriptase (Promega, Madison, WI) were applied in a total reaction volume of 25 μl. PCRs were performed with respective primers as described in Table 1 for 25 cycles in a thermal cycler (PTC-200, MJ Research, Waltham, MA) according to the following protocol: denaturation at 94°C for 30 s, annealing at 55~60°C for 30 s, and elongation at 72°C for 1 min, with ef1α as an internal control. PCR products were analyzed on 1.2% (w/v) agarose gels stained with ethidium bromide.

Riboprobe preparation and whole-mount *in situ* hybridization

PCR products with a complete ORF of zebrafish stathmins were cloned into the pGEM-T Easy Vector (Promega), and confirmed by sequencing. Antisense RNA riboprobes were synthesized using the digoxigenin RNA Labeling Kit (Roche Applied Science, Penzberg, Germany). Embryos were staged according to Kimmel et al. (1995) in hours post-fertilization (hpf), fixed in 4% paraformaldehyde in phosphate-buffered saline (PBS) at 4°C overnight, and then stored in methanol at -20°C until use. Whole-mount *in situ* hybridization was performed with respective antisense riboprobes as described previously (Thisse et al., 1993).

MO-mediated knockdown of stathmin2a expression

An anti-sense MO (tMO: 5'-CATGGTGTCGTTTCTTGAATCCGTA-3'), a 5 base pair mismatched (mis-MO: 5'-CATcGTcTCGTTTgTTcAATCCcTA-3') and a standard control MO (StdMO: 5'-CCTCTTACCTCAGTTACAATTTATA-3') were used to block translation of zebrafish *stathmin2a* by targeting at ATG site (GeneTools, Philomath, OR, USA). The MOs were re-suspended in sterile water at 1mM stock concentration. Immediately prior to injection, tMO and mis-tMO were diluted to 0.5 mM in embryonic medium with saturated phenol red (Sigma, Poole, UK) into the yolk cell of one- to four-cell stage embryos by using a Nanoliter 2000 injector (World Precision Inc., USA).

Embryo observations and photography

Observation of embryonic development and whole-mount ISH were made at designated times under a Leica Mz75 stereomicroscope (Heidelberg, Germany). All photographs were taken by a Nikon Coolpix 995 digital camera (Tokyo, Japan).

Preparation of stmn2a mRNA for rescue

The full length of *stmn2a* with 5 point mutations (show the mutated sites on Table S1) at the MO targeting site, which impairs its binding activity to the anti-sense MO, was cloned into the pcDNA vector. The capped mRNA were transcribed by T7 polymerase (mMESSAGE mMACHINE™, Ambion) and dissolved in nucleotide-free water. Embryos were injected with the capped mRNA with or without *stmn2a* MO to monitor its rescue effect.

RESULTS

Cloning and sequence analysis of zebrafish stathmin family genes

By *in silica* cloning, we identified candidate EST sequences or predicted transcripts for zebrafish orthologs of stathmin family genes. Using reverse-transcription polymerase chain reaction (RT-PCR), four stathmin family genes with a complete coding region were isolated from complementary (c)DNA pools of zebrafish embryos at various stages from 1-cell to 72 h post-fertilization (hpf). Sequences of primer sets used are listed in supplementary Table S1. These stathmin genes were named according to the Zebrafish Nomenclature Guidelines and approved by the Zebrafish Nomenclature Committee. The four cloned zebrafish stathmin orthologs are *stathmin 1b* (*stmn1b*), *stathmin-like 2a* (*stmn2a*), *stathmin-like 3* (*stmn3*), and *stathmin-like 4* (*stmn4*), which respectively correspond to mammalian *stathmin* (*Stmn1*), SCG10 (*Stmn2a*), SCLIP (*Stmn3*), and RB3 (*Stmn4*).

These *stathmin* genes are located in different chromosomes with variable sizes and genomic organization (Fig. 1A). Comparing their deduced amino acid sequences, we found that they share similar functional domain structures (Fig. 1 B). The conserved stathmin-like domain (SLD), a signature of stathmin, exists in all the four zebrafish stathmin orthologs. These SLDs, share 54%~67% sequence identities compared to Stmn1b (Fig. 1C). We identified several consensus phosphorylation sites in the SLDs (Fig.1B). According to the Stmn1b sequence, Ser18 and Ser48 are conserved

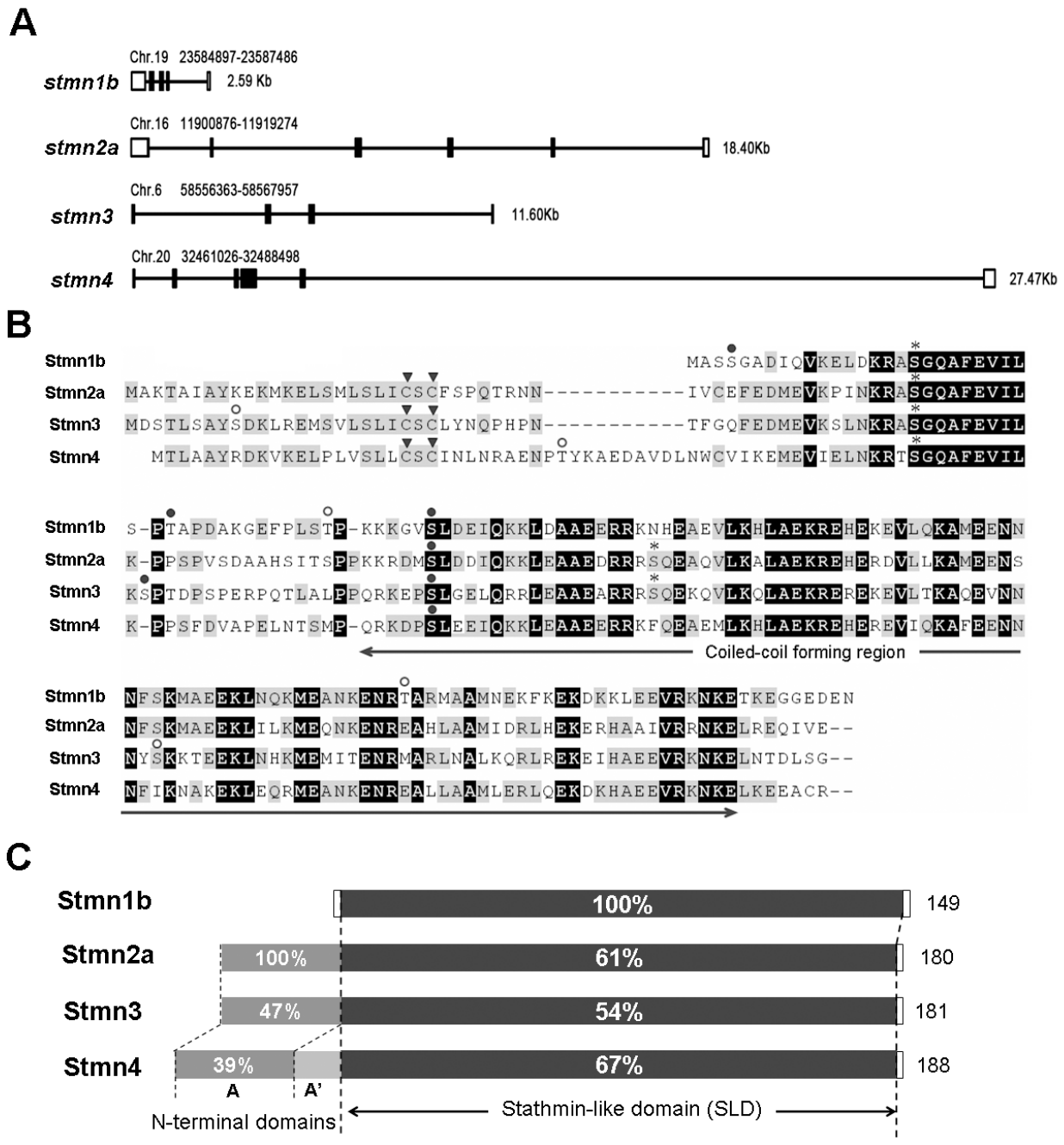

Fig. 1. Chromosomal location, sequence alignment, and domain analysis of zebrafish stathmins. A: Schematic depiction of *stmn1b*, *stmn2a*, *stmn3,* and *stmn4*, showing the chromosomal location (above), size (right), and organization (introns and exons are shown in empty and solid boxes, respectively). B: Sequence alignment of Stmn1b, Stmn2a, Stmn3, and Stmn4, showing identical amino acids on a black background, and similar amino acids on a gray background. The arrowheads (▼) point to the cysteine amino acids which may be palmitoylated; asterisks (*) predict potential cAMP- and cGMP-dependent protein kinase phosphorylation sites; open circles (○) indicate potential protein kinase C phosphorylation sites; and filled circles (●) designate potential casein kinase II phosphorylation sites. C: Structural domain organizations of Stmn1b, Stmn2a, Stmn3, and Stmn4, showing the respective length of amino acid residues for each protein on the right. In addition to the common stathmin-like domain (the percent (%) identity compared to Stmn1b is labeled for each protein) except for Stmn1b; each stathmin contains an N-terminal extension including the conserved domain A (dark gray, the % of identity compared with Stmn2a is labeled for each protein), and Stmn4 has an additional domain A' (light gray).

in all four stathmins. Those sites have the consensus domains for phosphorylation by cAMP/cGMP-dependent protein kinase and casein kinase II, respectively. A motif scan revealed that these SLDs have a predicted α-helical structure, which can potentially form a coiled-coil interaction with other proteins (Fig. 1B, http://smart.embl-heidelberg.de/). Similar to mammalian SCG10 family proteins, Stmn2a, Stmn3, and Stmn4 also contain a conserved N-terminal extension. Sequence comparisons showed that the A domain within N-terminal extension of Stmn3 and Stmn4 respectively share 47% and 39% sequence identities with Stmn2a (Fig. 1C). In addition, two cysteine residues residing in the N termini of the SCG10 subfamily (arrowheads, Fig.1B) may assist in membrane tethering partly through palmitoylation (Gavet et al., 2002).

Besides the four *stathmins* we cloned, duplicates of *stmn1*, *2,* and *4* were annotated in the NCBI zebrafish database during the period of our investigation. Comparing the deduced amino acid sequences of all these zebrafish stathmins (supplementary Table S2), we found that Stmn1b we cloned only differs in amino acid residue 46 (G) compared to the Stmn1b (NP_001017850, E) posted on ZFIN, which may be due to polymorphism or a PCR error (please see nucleotide and amino acid sequence alignments in supplementary Fig. S1). Since our PCR cloning used at least two different pools of cDNAs and obtained exactly the same nucleotide sequence, the mutations should not be due to PCR errors. Despite the minimal difference, we consider them to be the same gene, *stmn1b*, in this study. We also found that the Stmn1b shares 89% similarity with another stathmin isoform, Stmn1a (Table S2). The *stmn2a* gene we identified is *stmn2a*, which is clustered with zebrafish *stmn2b* (supplementary Fig. S2). There is only one annotated zebrafish *stmn3* sequence available, which is identical to the *stmn3* we cloned. The *stmn4* we cloned also differs in deduced amino acid residue 82 (M) compared to that of *stmn4* (NM_213401) with I, respectively, that has also been confirmed not to be due to PCR errors, so here we assume that they are the same gene, *stmn4* (please see nucleotide and amino acid sequence alignments in supplementary Fig. S3). We also found that the Stmn4 shares 84% similarity with another stathmin isoform, Stathmin 4-like (Stmn4l, Table S2).

To further analyze the divergence of stathmin family genes among vertebrates, the deduced amino acid sequences of zebrafish stathmins were compared to their putative orthologs of human (*Homo sapiens*), mouse (*Mus musculus*), and frog (*Xenopus lavis*), and their respective identity/similarity percentages are listed in supplementary Table S3. As shown in Table S3, all four zebrafish stathmins share high identity/similarity with their corresponding mammalian or amphibian orthologs. The phylogenetic tree analysis revealed that Stmn1, Stmn3, and Stmn4 are clustered with their corresponding proteins and demonstrated that they are orthologs of vertebrate stathmin family genes (Fig. S2).

Temporal and spatial expression pattern analyses of stathmins by RT-PCR

To examine the temporal expression patterns of stathmins during early development, we performed an RT-PCR analysis on zebrafish embryos at 11 different stages from the 1-cell stage to 72 hpf. Transcriptions of *stmn1b*, *stmn3,* and *stmn4* increased from their onset, but that of *stmn3* declined after 36 hpf. In contrast, *stmn2a* transcripts existed in all stages examined with stronger expression appearing after 48 hpf (Fig. 2A). Furthermore, to study the tissue-specific expression patterns we examined expressions of these stathmins in different adult tissues, including the brain, eyes, skin, skeletal muscles, ovaries, testes, kidneys, spleen, intestines, gills, heart, swim bladder, and liver. The *stmn1b* was expressed in all tissues examined with notably higher expression in the brain and eyes; *stmn2a* existed in the brain, eyes, ovaries, testes, and intestines; *stmn3* had higher expression in the brain and eyes, but lower expression in muscles; and *stmn4* was ubiquitously expressed in all tissues examined, but had lower expressions in the skin and liver (Fig. 2B).

Expression pattern analyses of stathmins by whole-mount in situ hybridization

The expressions of zygotic *stathmin*s, besides *stmn2a,* were activated at around 16 hpf. Since this is about the time of initiation of neurogenesis in zebrafish, we further examined the spatial expressions of *stathmins* in the nervous system of embryos collected from 16 to 72 hpf by whole-mount *in situ* hybridization. During segmentation stages, all *stathmins* examined were present in spinal cord neurons (arrows) and trigeminal ganglia/cranial ganglia (arrowheads, Fig. 3). By examining the available expression patterns for other *stathmins* (*stmn1a*, *stmn1b*, *stmn2b*, *stmn4*, and *stmn4l*) on the Zebrafish Information Network (ZFIN, University of Oregon, Eugene, OR; URL: http://zfin.org/), their expression patterns in the central nervous system (CNS) along with those of stathmins cloned in this study are summarized in Fig. S4. Since the expression patterns of *stmn1b* and *stmn4* were quite similar between ours and the corresponding data on ZFIN, only our data are included here. We found that *stmn1a* and *stmn2b,* but not *stmn4l*, were expressed in spinal cord neurons and trigeminal ganglia/cranial ganglia (Fig. S4A). After brain regionalization takes

place (~18 hpf), the expressions of *stmn1b*, *stmn2a,* and *stmn3* expanded to the CNS (Figs. 3E-G, E'-G'), but not that of *stmn4* (Figs. 3H, H'). We noted that transcripts of *stmn1b* and *stmn2a* are weak in the brain region before 24 hpf, but are increased thereafter (Figs. 3, 4). In contrast, *stmn1a* (Fig. S4) was highly expressed in the anterior portion of embryos in particular in the eyes, midbrain, hindbrain, and neural tube at 16 hpf, and the entire CNS was darkly stained at 24~25 hpf, which might be overstained, but it nonetheless indicated high expression in these regions. In addition, the expression of *stmn2b* was strong in spinal cord neurons and the midbrain region around 18 hpf (Fig. S4). The expression patterns of *stmn4* and *stmn4l* greatly differed during the segmentation stages; *stmn4* was barely detected during 16~18 hpf (Fig. 3), but *stmn4l* obviously appeared in some brain regions and spinal cord neurons (Fig. S4).

At early larval stages, *stmn1b* was strongly expressed in the telecephalon, diencephalon, midbrain, hindbrain rhomobomeres, and cranial ganglia, including the trigeminal ganglion, anterior lateral line ganglion, and posterior lateral line ganglion at 24 hpf (Figs. 3M, M', S4). In the cerebellum, *stmn1b* expression was weak at 24 hpf, but stronger after 36 hpf. The distribution of *stmn1b* transcripts extended to the thalamus in the midbrain region after 36 hpf, and to the retina and tectum opticum in the anterior head region after 48 hpf. The expression of *stmn1b* in the otic vesicle was weak at 36 hpf, but persisted until 72 hpf (Figs. 4A, A', E, E', F, F'). In contrast to the restricted *stmn1b* expression domains, transcripts of *stmn1a* were found in the entire brain from initiation of nervous system development, and its expression in the spinal cord persisted throughout embryonic development (Fig. S4).

Distributions of *stmn2a* transcripts in the brain region at 24~48 hpf were similar to those of *stmn1b,* but it was not detected in the tectum opticum or cerebellum, and was denser in hindbrain rhomobomeres (Figs. 3N, N', 4B, B', F, F'). Its expression in the retina was weak at 36 hpf, but strengthened to 72 hpf (Figs. 4B, B', F, F', stars in J, J').

We are the first group to identify the zebrafish ortholog of mammalian *stathmin 3*, and we obtained approval from the zebrafish nomenclature committee to name it *stathmin-like 3* (*stmn3*). Unlike *stmn1b* and *stmn2a*, the expression of *stmn3* was strong and restricted to spinal cord neurons, hindbrain regions (including rhomobomeres and cranial ganglia), and the tegmentum during the late segmentation and early larval stages. In contrast, *stmn3* transcripts were barely detected in the forebrain, midbrain, and cerebellum regions, except for the thalamus and tegmentum (Figs. 3O, O', 4C, C', G, G', K, K', S4).

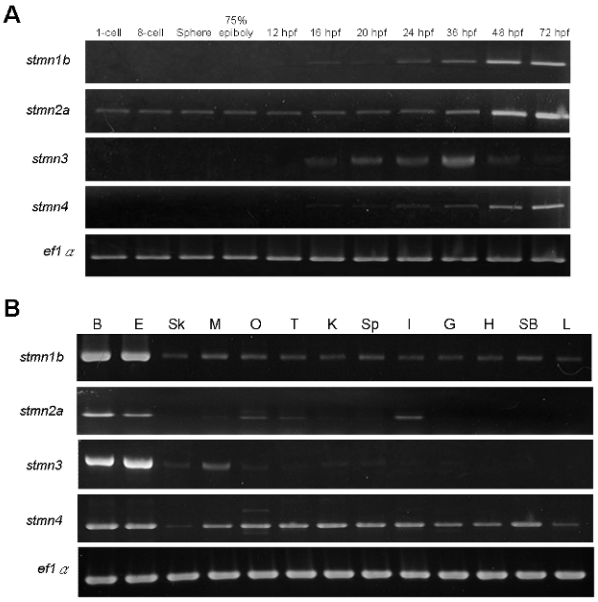

Fig. 2. RT-PCR analysis showing the expression patterns of stathmin family genes. A: Expressions of zebrafish *stmn1b, stmn2a, stmn3,* and *stmn4* during embryonic and larvae stages. B: Distributions of *stmn1b, stmn2a, stmn3,* and *stmn4* mRNAs in adult tissues. B, brain; E, eyes; Sk, skin; M, skeletal muscles; O, ovaries; T, testes; K, kidneys; Sp, spleen; I, intestines; G, gills; H, heart; SB, swim bladder; L, liver. The *ef1α* gene was used as an internal control for the homogeneity of cDNA samples.

Although transcripts of *stmn4* were also found in the CNS and spinal cord neurons among all stages examined, its signal was much weaker and less distinct than those of other stathmin family genes (Figs. 3P, P', 4D, D', H, H', L, L'). Only signals in the tegmentum, thalamus, and cranial ganglia were obviously recognized at 24~36 hpf in embryos hybridized with *stmn4* antisense riboprobes (Figs. 3P, P', 4D, D'). In addition, *stmn4* was also expressed in the pectoral fin after 48 hpf (Fig 4H, H', L, L'). The distribution of *stmn4l* transcripts was distinct from that of *stmn4*, especially in early larva stages; *stmn4* was weak and widely distributed, but *stmn4l* transcripts were obviously restricted to the forebrain, hindbrain, tegmentum, and hypothalamus (Fig. S4).

Down-regulation of Stmn2a causes brain edema and reduction in brain size

Due to the specific expression of stathmins in different domains of the central nerve system, it implies that stathmins may play distinct roles in CNS development. To test this hypothesis, we knocked down one of the stathmins, *stmn2a* by an antisense morpholino oligonucleotide to block its translation

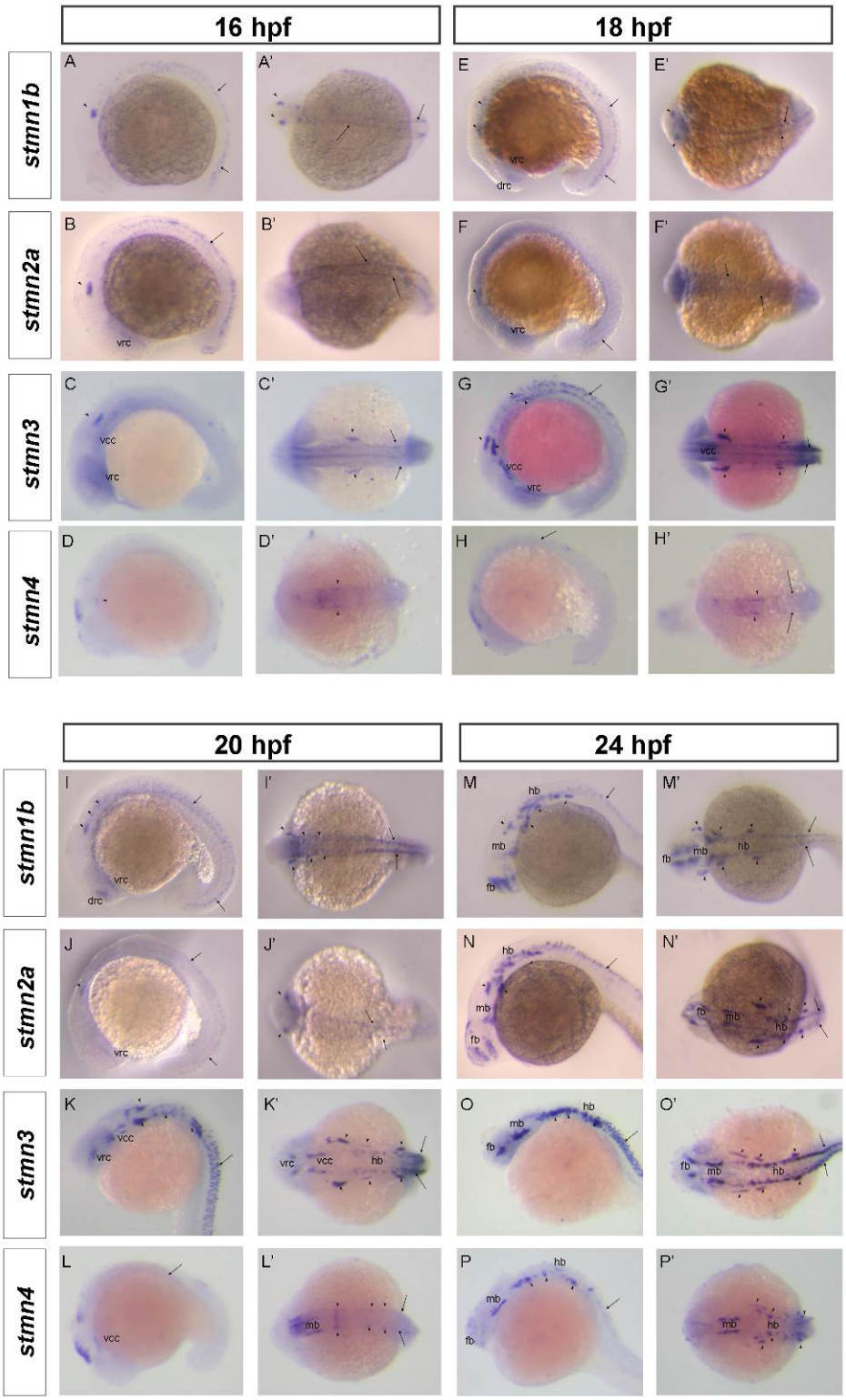

Fig. 3. Spatial expression of stathmin family genes in zebrafish during segmentation stages. Representative whole-mount *in situ* hybridization shows expression patterns of *stmn1b, stmn2a, stmn3,* and *stmn4* at the respective stages: A~D, A'~D', 16 h post-fertilization (hpf); E~H, E'~H', 18 hpf; I~L, I'~L', 20 hpf; M~P, M'~P', 24 hpf. A~P, lateral view; A'~P', dorsal view. Different organs or structures are indicated or labeled as follows: trigeminal placode (16 hpf, arrowhead) cranial ganglia (arrowhead), dorsorostral cluster (drc), forebrain (fb), hindbrain (hb), midbrain (mb), spinal cord neurons (arrow), ventrocaudal cluster (vcc), and ventrorostral cluster (vrc).

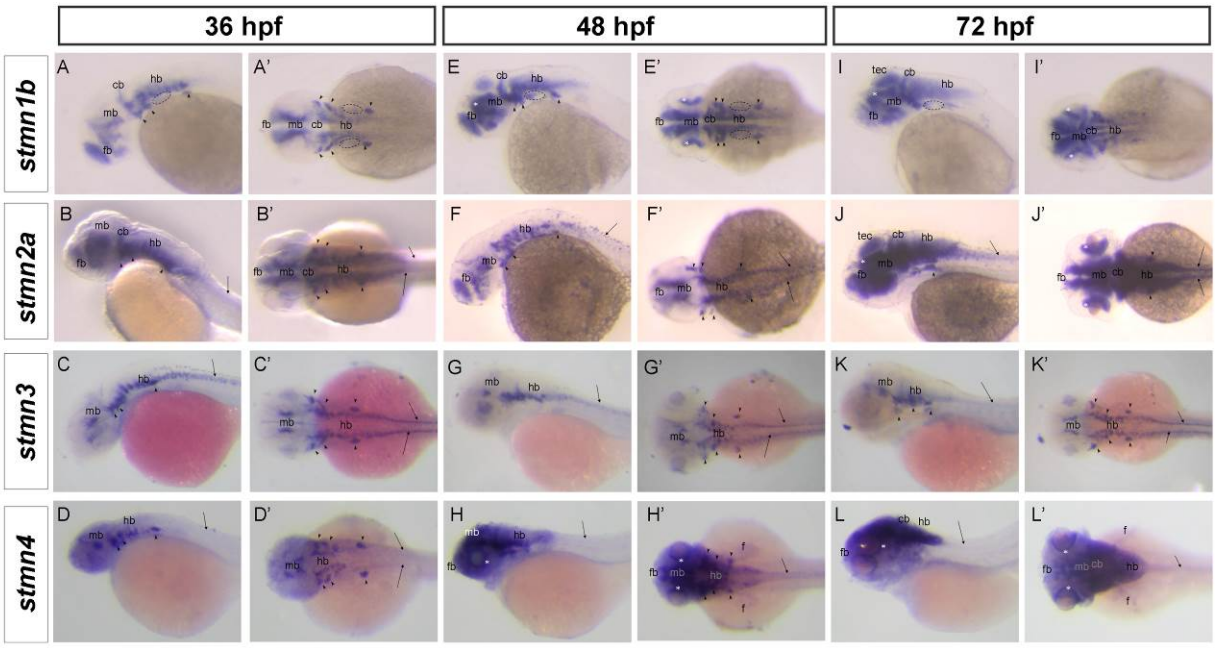

Fig. 4. Spatial expressions of stathmin family genes in zebrafish during early larval stages. Representative whole-mount *in situ* hybridization showing expression patterns of *stmn1b, stmn2a, stmn3,* and *stmn4* at respective stage: A~D, A'~D', expression in the nervous system at 36 h post-fertilization (hpf); E~H, E'~H', expression in the anterior region at 48 hpf; I~L, I'~L', expression in the head region at 72 hpf. A~L, lateral view; A'~L', dorsal view. Different organs or structures are indicated or labeled as follows: cerebellum (cb), cranial ganglia (arrowhead), fin (f), forebrain (fb), hindbrain (hb), midbrain (mb), otic vesicle (dotted circle), retina (asterisk), spinal cord neurons (arrow), and tectum opticum (tec).

(tMO). The *stmn2a* tMO efficiently and specifically blocks the green fluorescent protein (GFP) expression in zebrafish embryos co-injected with a pCS2+ vector harboring a partial *stmn2a* sequence containing its MO targeting site. In contrast, a 5 base pair mis-matched *stmn2a* MO (mis-MO) co-injected embryos showed strong mosaic GFP fluorescence as that in embryos-injected with the *stmn2a* plasmid only (Fig. 5). We observed narrow midbrain-hindbrain boundary (arrowhead in Fig. 6) and hindbrain edema (arrow in Fig. 6) in *stmn2a* MO-injected larva at 24 and 48 hpf compared to the normal brain morphology in untreated and standard control MO-injected embryos (Fig. 6). These *stmn2a* tMO-induced defects were specific due to the loss of Stmn2a since these brain defects could not seen in mis-MO-injected embryos and could be rescued by co-injected 50 pg *stmn2a* mRNA (Fig. 6 E, E', J, J'). In 4 ng tMO-treated larvae, about one-quarter of the larvae died at 28 hpf and increased continuously after 24 hours; in contrast, larvae co-injected with 50 pg *stmn2a* mRNA showed less death and defects (Fig. 6 K, L) during 28 and 48 hpf.

To further examine *stmn2a* regulation on neurogenesis, an early neural marker *islet1* (*isl1*) was used by visualize early neural differentiation of development (Inoue et al., 1994; Korzh et al., 1993). Dorsal and lateral views of *isl1* mRNA expression are shown during 36 and 48 hpf, respectively (Fig. 7A, A', E and E', respectively). In control and standard MO-treated larvae, *isl1* transcripts appeared in forebrain nuclei, trigeminal ganglia, and branchiomotor neuron of hindbrain neurons at 36 hpf and high level of expression showed in retina ganglion and inner cell layer and several brain nuclei at 48 hpf. In contrast, clear reduction in *isl1* expression was observed in larvae treated with 4 ng *stamn2* tMO at 48 hpf.

DISCUSSION

In this study, we identified and cloned four stathmin genes: *stathmin 1b* (*stmn1b*), *stathmin-like 2a* (*stmn2a*), *stathmin-like 3* (*stmn3*), and *stathmin-like 4* (*stmn4*). Their sequences were analyzed and their expression patterns, particularly neuronal expression, were investigated. By sequence analysis, we confirmed that all zebrafish stathmins cloned have a characteristic stathmin-like domain (SLD). In addition, zebrafish SCG10 family proteins, including Stmn2a, Stmn3 and Stmn4, also have a short stretch of NH2-terminal domain for membrane interaction like their mammalian homologs (Charbaut et al., 2005; Ozon et al., 1997). Furthermore, these zebrafish stathmin proteins share

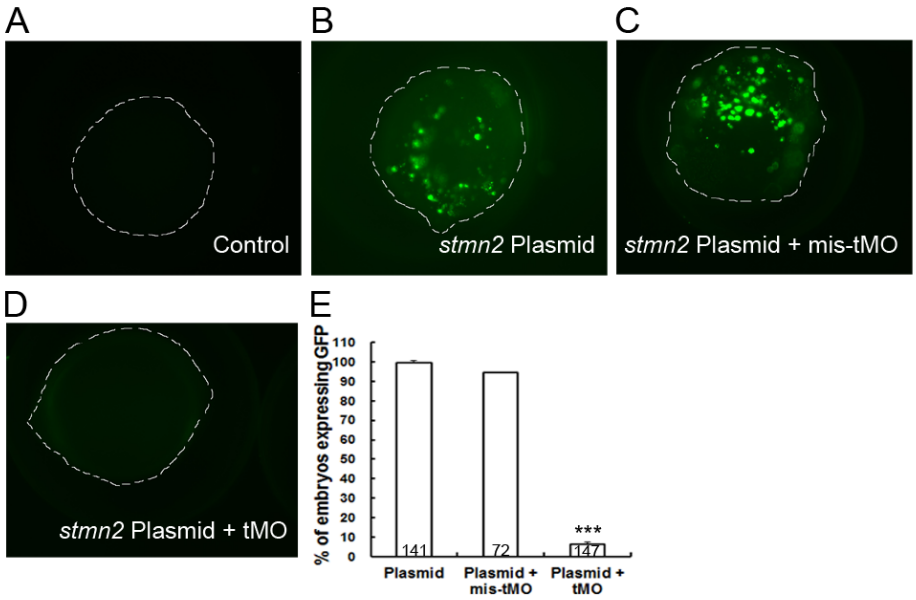

Fig. 5. *stmn2a* tMOs efficiency check. A plasmid containing 100 pg *stmn2a* MO binding site and enhanced green fluorescent protein (EGFP) were un-injected (A) or injected into 1-cell stage embryos without (B) or with *stmn2a* mis-tMO (C) or *stmn2a* tMO (D). Percentages of embryos showing EGFP fluorescence are shown in different treatments in (E). Numbers of embryo examined are shown at the bottom of each bar. *** $p < 0.0001$.

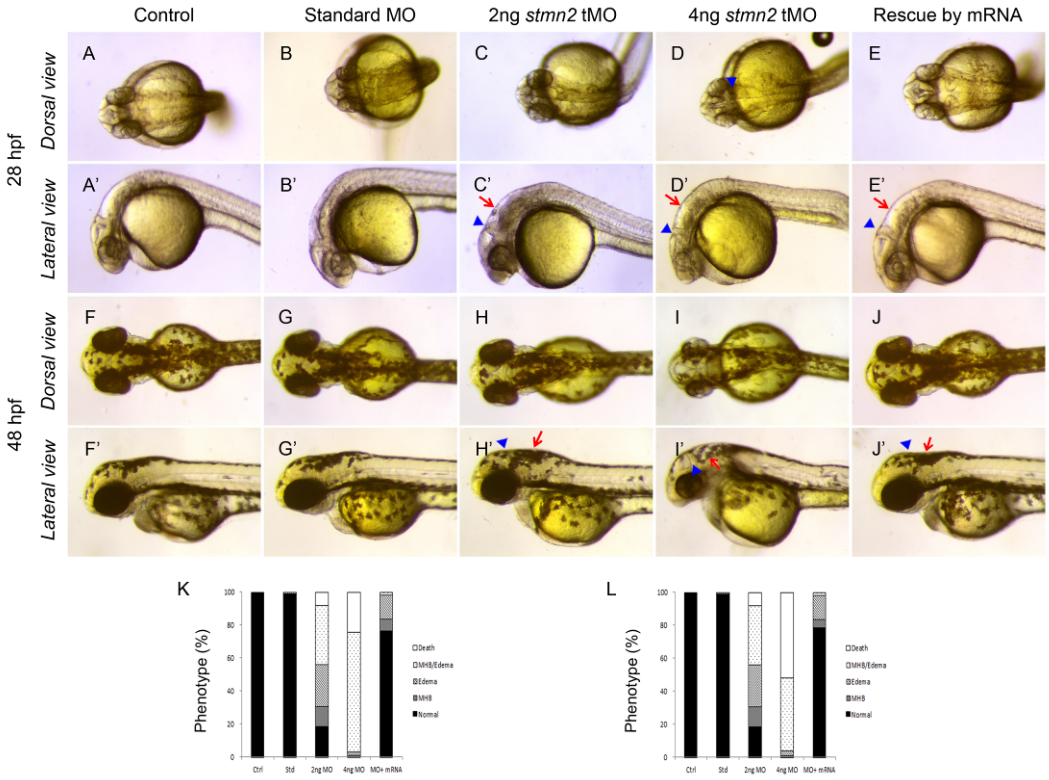

Fig. 6. Knockdown of *stmn2a* impairs brain development. 1-cell stage embryos were injected without (control) or with indicated MO and *stmn2* mRNA, cultured to the designated time and photographed at the dorsal and lateral views. Representative photographs are shown for each treatment. Each treatment used 98 embryos. *Stmn2a* MO-injected embryos showed edema in the hindbrain ventricle (arrow), a narrow midbrain-hindbrain boundary (arrowhead) and hindbrain opacity. K, L show statistical analysis for indicated phenotypes at 28 and 48 hpf, respectively. Black bars indicate normal morphology; meshed bars show narrow midbrain-hindbrain boundary (MHB); twilled bars exhibit hindbrain edema; and open bars are dead larvae. All data represent at least three independent experiments.

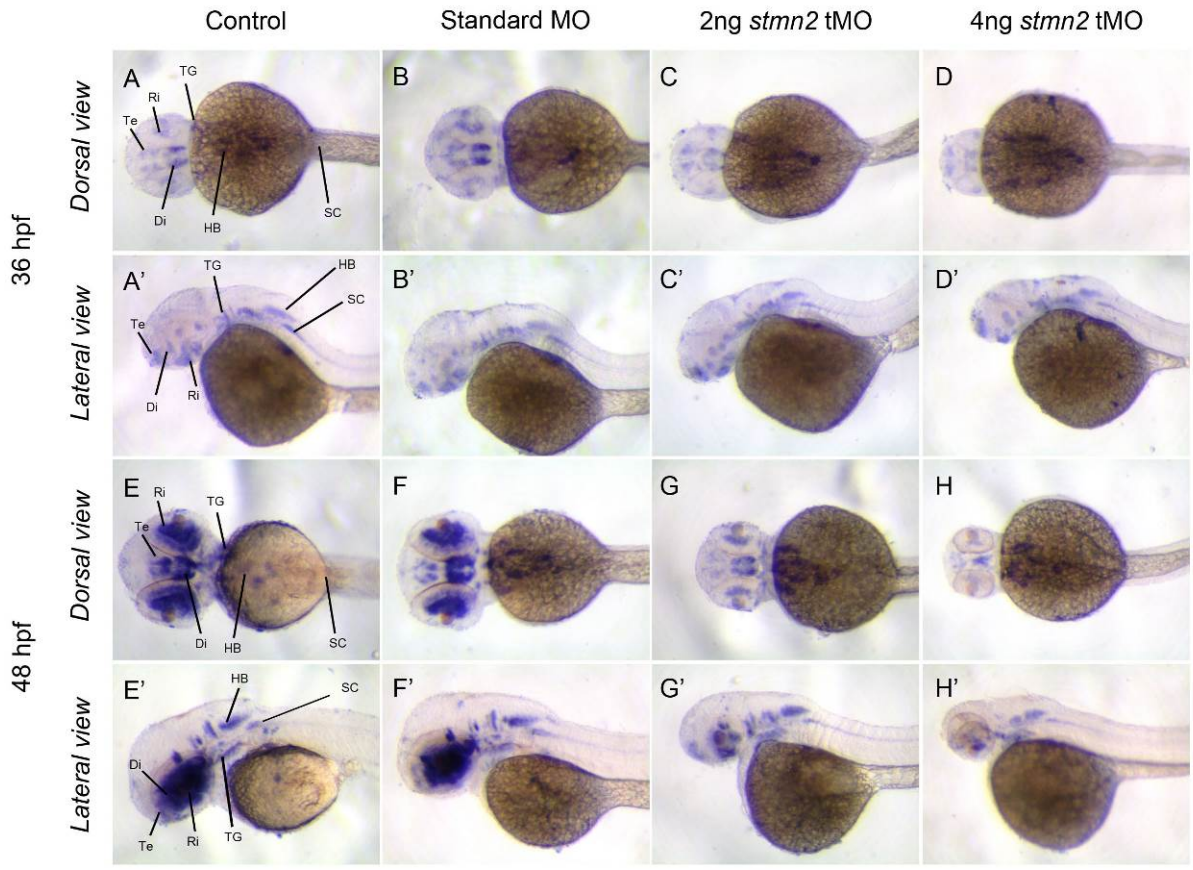

Fig. 7. Knockdown of *stmn2a* inhibits *islet1* expression. 1-cell stage embryos were injected without (control) or with indicated MO, fixed at designated time, subjected to whole-mount *in situ* hybridization and photographed at the dorsal and lateral views. Representative photographs are shown for each treatment. Labels used: diencephalon (Di), hindbrain (HB), retina (Ri), spinal cord (SC), telencephalon (Te) and trigeminal ganglion (TG).

characteristics phosphorylation sites as their homologs from other species like human, drosophila and mouse (Charbaut et al., 2001; Ozon et al., 2002).

We observed dynamic and spatially restricted expression patterns of zebrafish stathmin family genes, including *stmn2a*. Similar observations have also been reported for both zebrafish *stmn2a* and *stmn2b* (Burzynski et al., 2009) and rat stathmin (Ozon et al., 1999). All stathmins studied have a strong expression in the brain and spinal cord at later stage (36-72 hpf). This implies that stathmins are highly related to CNS development and may have distinct roles due to their different expression domains during developmental stage. Zebrafish stathmin family genes initiate expression at different embryonic stages. Only *stmn2a* expresses throughout development, other stathmins begin to be expressed after 16 hpf. This suggests that *stmn2a* may play a more important role compared to other stathmins during early development.

The consistent expression of *stmn2a* during early embryogenesis drew our attention to investigate its roles during early development. We show here the specific and effective knockdown of *stmn2a* expression. More importantly, the loss of Stmn2a results in brain development defects. A recent report showed that knockdown of both *stmn2a* and *stmn2b* only show developmental delay, which is different from our observations (Alves et al., 2010). However, the splicing blocking MOs have no inhibition on the translation of existing mRNA. In addition, the splicing blocking effects of *stmn2a* MOs used by them was not shown in the paper. In contrast, we clearly show the efficacy of the translational blocking MO to block *stmn2a* translation (Fig. 5). Together, we conclude that *stmn2a* gene is an essential modulator of temporal expression of brain formation in the zebrafish.

The inhibition of *stmn2a* MO on the formations of midbrain-hindbrain boundary and hindbrain raises the

possibility that *stmn2a* regulates the progressive events of those tissue regions. Our results show that formation of hindbrain is particularly sensitive to *stmn2a* knockdown at 48 hpf. These data suggest that *stmn2a* similarly modulates relationship among hindbrain formation signaling during embryogenesis, and offer an explanation for the *stmn2a* MO-induced defects. These results coincide well with the central role of *stmn2a* during brain development in other vertebrates (Pellier-Monnin et al., 2001; Sugiura and Mori, 1995; Westerlund et al., 2011) and its importance in neuron outgrowth and axon guidance development (Grenningloh et al., 2004; Morii et al., 2006; Suh et al., 2004).

In summary, we isolated and characterized theexpression patterns of four zebrafish stathmin family orthologs: *stathmin 1b* (*stmn1b*), *stathmin-like 2a* (*stmn2a*), *stathmin-like 3* (*stmn3*), and *stathmin-like4* (*stmn4*). Together with previously identified *stathmin 1a* (*stmn1a*) and *stathmin-like 4, like* (*stmn4l*), we found that these genes are mainly expressed in the CNS with distinct expression domains. The divergent temporal and spatial expressions of zebrafish *stathmins* imply that these orthologs may be involved in different aspects of regulating formation of the nervous system, especially the CNS, during embryogenesis in zebrafish. We and others show the requirement of *stmn2a* in CNS development and the roles of other sthathmins await further investigation.

LITERATURE CITED

Alves, M. M., G. Burzynski, J. M. Delalande, J. Osinga, A. van der Goot, A. M. Dolga, . . . R. M. Hofstra. 2010. Kbp interacts with scg10, linking goldberg-shprintzen syndrome to microtubule dynamics and neuronal differentiation. Hum. Mol. Genet. 19: 3642–3651. doi: 10.1093/hmg/ddq280

Anderson, D. J. and R. Axel. 1985. Molecular probes for the development and plasticity of neural crest derivatives. Cell 42: 649–662.

Belmont, L., T. Mitchison and H. W. Deacon. 1996. Catastrophic revelations about op18/stathmin. Trends Biochem. Sci. 21: 197–198.

Beretta, L., T. Dobransky and A. Sobel. 1993. Multiple phosphorylation of stathmin. Identification of four sites phosphorylated in intact cells and in vitro by cyclic amp-dependent protein kinase and p34cdc2. J. Bio. Chem. 268: 20076–20084.

Bieche, I., A. Maucuer, I. Laurendeau, S. Lachkar, A. J. Spano, A. Frankfurter, . . . P. A. Curmi. 2003. Expression of stathmin family genes in human tissues: Non-neural-restricted expression for sclip. Genomics 81: 400–410.

Bouquet, C. and F. Nothias. 2007. Molecular mechanisms of axonal growth. Adv. Exp. Med. Biol. 621: 1–16. doi: 10.1007/978-0-387-76715-4_1

Brattsand, G., U. Marklund, K. Nylander, G. Roos and M. Gullberg. 1994. Cell-cycle-regulated phosphorylation of oncoprotein 18 on ser16, ser25 and ser38. Eur. J. Biochem. / FEBS 220: 359–368.

Burzynski, G. M., J. M. Delalande and I. Shepherd. 2009. Characterization of spatial and temporal expression pattern of scg10 during zebrafish development. Gene expression patterns: GEP 9: 231–237. doi: 10.1016/j.gep .2008.12.010

Charbaut, E., P. A. Curmi, S. Ozon, S. Lachkar, V. Redeker and A. Sobel. 2001. Stathmin family proteins display specific molecular and tubulin binding properties. J. Biol. Chem. 276: 16146–16154. doi: 10.1074/jbc.M010637200

Charbaut, E., S. Chauvin, H. Enslen, S. Zamaroczy and A. Sobel. 2005. Two separate motifs cooperate to target stathmin-related proteins to the golgi complex. J. Cell Sci. 118: 2313–2323. doi: 10.1242/jcs.02349

Chauvin, S., F. E. Poulain, S. Ozon and A. Sobel. 2008. Palmitoylation of stathmin family proteins domain a controls golgi versus mitochondrial subcellular targeting. Biology of the cell / under the auspices of the European Cell Biology Organization 100: 577–589. doi: 10.1042/BC20070119

Chneiweiss, H., J. Cordier and A. Sobel. 1992. Stathmin phosphorylation is regulated in striatal neurons by vasoactive intestinal peptide and monoamines via multiple intracellular pathways. J. Neurochem. **58:** 282–289.

Curmi, P. A., A. Maucuer, S. Asselin, M. Lecourtois, A. Chaffotte, J. M. Schmitter and A. Sobel. 1994. Molecular characterization of human stathmin expressed in escherichia coli: Site-directed mutagenesis of two phosphorylatable serines (ser-25 and ser-63). The Biochemical journal **300 (Pt 2):** 331–338.

Desai, A. and T. J. Mitchison. 1997. Microtubule polymerization dynamics. Annu. Rev. Cell Dev. Biol. **13:** 83–117. doi: 10.1146/annurev.cellbio.13.1.83

Doye, V., M. C. Boutterin and A. Sobel. 1990. Phosphorylation of stathmin and other proteins related to nerve growth factor-induced regulation of pc12 cells. J. Biol. Chem. **265:** 11650–11655.

Gavet, O., S. Ozon, V. Manceau, S. Lawler, P. Curmi and A. Sobel. 1998. The stathmin phosphoprotein family: Intracellular localization and effects on the microtubule network. J. Cell Sci. **111 (Pt 22):** 3333–3346.

Gavet, O., S. El Messari, S. Ozon and A. Sobel. 2002. Regulation and subcellular localization of the microtubule-destabilizing stathmin family phosphor- proteins in cortical neurons. J. Neurosci. Res. **68:** 535–550. doi: 10.1002/jnr.10234

Gigant, B., F. Iseni, Y. Gaudin, M. Knossow and D. Blondel. 2000. Neither phosphorylation nor the amino-terminal part of rabies virus phosphoprotein is required for its oligomerization. J. Gen. Virol. **81:** 1757–1761.

Grenningloh, G., S. Soehrman, P. Bondallaz, E. Ruchti and H. Cadas. 2004. Role of the microtubule destabilizing proteins scg10 and stathmin in neuronal growth. J. Neurobiol. **58:** 60–69. doi: 10.1002/neu.10279

Himi, T., T. Okazaki, H. Wang, T. H. McNeill and N. Mori. 1994. Differential localization of scg10 and p19/stathmin messenger rnas in adult rat brain indicates distinct roles for these growth-associated proteins. Neuroscience **60:** 907–926.

Inoue, A., M. Takahashi, K. Hatta, Y. Hotta and H. Okamoto. 1994. Developmental regulation of islet-1 mrna expression during neuronal differentiation in embryonic zebrafish. Dev. Dynam. **199:** 1–11. doi: 10.1002/aja.1001990102

Jourdain, L., P. Curmi, A. Sobel, D. Pantaloni and M. F. Carlier. 1997. Stathmin: A tubulin-sequestering protein which forms a ternary t2s complex with two tubulin molecules. Biochemistry **36:** 10817–10821. doi: 10.1021/bi971491b

Kline-Smith, S. L. and C. E. Walczak. 2004. Mitotic spindle assembly and chromosome segregation: Refocusing on microtubule dynamics. Mol. Cell **15:** 317–327. doi: 10.1016/j.molcel.2004.07.012

Koppel, J., M. C. Boutterin, V. Doye, H. Peyro-Saint-Paul and A. Sobel. 1990. Developmental tissue expression and phylogenetic conservation of stathmin, a phosphoprotein associated with cell regulations. J. Biol. Chem. **265:** 3703–3707.

Korzh, V., T. Edlund and S. Thor. 1993. Zebrafish primary neurons initiate expression of the lim homeodomain protein isl-1 at the end of gastrulation. Development **118:** 417–425.

Larsson, N., H. Melander, U. Marklund, O. Osterman and M. Gullberg. 1995. G2/m transition requires multisite phosphorylation of oncoprotein 18 by two distinct protein kinase systems. J. Biol. Chem. **270:** 14175–14183.

Lawler, S., O. Gavet, T. Rich and A. Sobel. 1998. Stathmin overexpression in 293 cells affects signal transduction and cell growth. FEBS letters **421:** 55–60.

Leighton, I. A., P. Curmi, D. G. Campbell, P. Cohen and A. Sobel. 1993. The phosphorylation of stathmin by map kinase. Mol. Cell. Biochem. **127-128:** 151–156.

Liedtke, W., E. E. Leman, R. E. Fyffe, C. S. Raine and U. K. Schubart. 2002. Stathmin-deficient mice develop an age-dependent axonopathy of the central and peripheral nervous systems. Am. J. Pathol. **160:** 469–480. doi: 10.1016/S0002-9440(10)64866-3

Luo, X. N., B. Mookerjee, A. Ferrari, S. Mistry and G. F. Atweh. 1994. Regulation of phosphoprotein p18 in leukemic cells. Cell cycle regulated phosphorylation by p34cdc2 kinase. J. Biol. Chem. **269:** 10312–10318.

Lutjens, R., M. Igarashi, V. Pellier, H. Blasey, G. Di Paolo, E. Ruchti, . . . G. Grenningloh. 2000. Localization and targeting of scg10 to the trans-golgi apparatus and growth cone vesicles. Eur. J. Neurosci. **12:** 2224–2234.

Manceau, V., O. Gavet, P. Curmi and A. Sobel. 1999. Stathmin interaction with hsc70 family proteins. Electrophoresis **20:** 409–417. doi: 10.1002/(SICI)1522-2683(19990201)20:2<409::AID-ELPS409>3.0.CO;2-N

Manna, T., D. Thrower, H. P. Miller, P. Curmi and L. Wilson. 2006. Stathmin strongly increases the minus end catastrophe frequency and induces rapid treadmilling of bovine brain microtubules at steady state in vitro. J. Biol. Chem. **281:** 2071–2078. doi: 10.1074/jbc.M510661200

Marklund, U., G. Brattsand, O. Osterman, P. I. Ohlsson and M. Gullberg. 1993. Multiple signal transduction pathways induce phosphorylation of serines 16, 25, and 38 of oncoprotein 18 in t lymphocytes. J. Biol. Chem. **268:** 25671–25680.

Marklund, U., O. Osterman, H. Melander, A. Bergh and M. Gullberg. 1994. The phenotype of a "cdc2 kinase target site-deficient" mutant of oncoprotein 18 reveals a role of this protein in cell cycle control. J. Biol. Chem. **269:** 30626–30635.

Matsuo, N., S. Kawamoto, K. Matsubara and K. Okubo. 1998. A novel scg10-related gene uniquely expressed in the nervous system. Gene **215:** 477–481.

Maucuer, A., V. Doye and A. Sobel. 1990. A single amino acid difference distinguishes the human and the rat sequences of stathmin, a ubiquitous intracellular phosphoprotein associated with cell regulations. FEBS letters **264:** 275–278.

Maucuer, A., J. Moreau, M. Mechali and A. Sobel. 1993. Stathmin gene family: Phylogenetic conservation and developmental regulation in xenopus. J. Biol. Chem. **268:** 16420–16429.

Maucuer, A., J. H. Camonis and A. Sobel. 1995. Stathmin interaction with a putative kinase and coiled-coil-forming protein domains. PNAS **92:** 3100–3104.

Morii, H., Y. Shiraishi-Yamaguchi and N. Mori. 2006. Scg10, a microtubule destabilizing factor, stimulates the neurite outgrowth by modulating microtubule dynamics in rat hippocampal primary cultured neurons. J. Neurobiol. **66:** 1101–1114. doi: 10.1002/neu.20295

Okazaki, T., C. Nakanishi-Ito, N. Seo, T. Tanino, M. Takiguchi and K. Egawa. 1993. Recognition of the qa-2k tumor antigen by t cell receptor gamma/delta of an immunopotentiator-induced tumoricidal t cell of mice. Cancer immunology, immunotherapy : CII **36:** 83–88.

Ozon, S., A. Maucuer and A. Sobel. 1997. The stathmin family -- molecular and biological characterization of novel mammalian proteins expressed in the nervous system. Eur. J. Biochem. / FEBS **248:** 794–806.

Ozon, S., T. Byk and A. Sobel. 1998. Sclip: A novel scg10-like protein of the stathmin family expressed in the nervous system. J. Neurochem. **70:** 2386–2396.

Ozon, S., S. El Mestikawy and A. Sobel. 1999. Differential, regional, and cellular expression of the stathmin family transcripts in the adult rat brain. J. Neurosci. Res. **56:** 553–564.

Ozon, S., A. Guichet, O. Gavet, S. Roth and A. Sobel. 2002. Drosophila stathmin: A microtubule-destabilizing factor involved in nervous system formation. Mol. Biol. Cell **13:** 698–710. doi: 10.1091/mbc.01-07-0362

Pellier-Monnin, V., L. Astic, S. Bichet, B. M. Riederer and G. Grenningloh. 2001. Expression of scg10 and stathmin proteins in the rat olfactory system during development and axonal regeneration. J. Comp. Neurol. **433:** 239–254.

Peschanski, M., E. Hirsch, I. Dusart, V. Doye, S. Marty, V. Manceau and A. Sobel. 1993. Stathmin: Cellular localization of a major phosphoprotein in the adult rat and human cns. J. Comp. Neurol. **337:** 655–668. doi: 10.1002/cne.903370410

Redeker, V., S. Lachkar, S. Siavoshian, E. Charbaut, J. Rossier, A. Sobel and P. A. Curmi. 2000. Probing the native structure of stathmin and its interaction domains with tubulin. Combined use of limited proteolysis, size exclusion chromatography, and mass spectrometry. J. Biol. Chem. **275:** 6841–6849.

Schubart, U. K., M. D. Banerjee and J. Eng. 1989. Homology between the cdnas encoding phosphoprotein p19 and scg10 reveals a novel mammalian gene family preferentially expressed in developing brain. DNA **8:** 389–398.

Schubart, U. K., J. Xu, W. Fan, G. Cheng, H. Goldstein, G. Alpini, . . . et al. 1992. Widespread differentiation stage-specific expression of the gene encoding phosphoprotein p19 (metablastin) in mammalian cells. Differentiation; research in biological diversity **51:** 21–32.

Schubart, U. K., J. Yu, J. A. Amat, Z. Wang, M. K. Hoffmann and W. Edelmann. 1996. Normal development of mice lacking metablastin (p19), a phosphoprotein implicated in cell cycle regulation. J. Biol. Chem. **271:** 14062–14066.

Shumyatsky, G. P., G. Malleret, R. M. Shin, S. Takizawa, K. Tully, E. Tsvetkov, . . . V. Y. Bolshakov. 2005. Stathmin, a gene enriched in the amygdala, controls both learned and innate fear. Cell **123:** 697–709. doi: 10.1016/j.cell.2005.08.038

Sobel, A., M. C. Boutterin, L. Beretta, H. Chneiweiss, V. Doye and H. Peyro-Saint-Paul. 1989. Intracellular substrates for extracellular signaling. Characterization of a ubiquitous, neuron-enriched phosphoprotein (stathmin). J. Biol. Chem. **264:** 3765–3772.

Stein, C. A., K. Mori, S. L. Loke, C. Subasinghe, K. Shinozuka, J. S. Cohen and L. M. Neckers. 1988. Phosphorothioate and normal oligodeoxyribonucleotides with 5'-linked acridine: Characterization and preliminary kinetics of cellular uptake. Gene **72:** 333–341.

Strahler, J. R., N. Hailat, B. J. Lamb, K. P. Rogers, J. A. Underhill, R. F. Melhem, . . . et al. 1992. Activation of resting peripheral blood lymphocytes through the t cell receptor induces rapid phosphorylation of op18. J. Immunol. **149:** 1191–1198.

Sugiura, Y. and N. Mori. 1995. Scg10 expresses growth-associated manner in developing rat brain, but shows a different pattern to p19/stathmin or gap-43. Brain research. Dev. Brain Res. **90:** 73–91.

Suh, L. H., S. F. Oster, S. S. Soehrman, G. Grenningloh and D. W. Sretavan. 2004. L1/laminin modulation of growth cone response to ephb triggers growth pauses and regulates the microtubule destabilizing protein scg10. J. Neurosci. **24:** 1976–1986. doi: 10.1523/JNEUROSCI .1670-03.2004

Thisse, C., B. Thisse, T. F. Schilling and J. H. Postlethwait. 1993. Structure of the zebrafish snail1 gene and its expression in wild-type, spadetail and no tail mutant embryos. Development **119:** 1203–1215.

Westerlund, N., J. Zdrojewska, A. Padzik, E. Komulainen, B. Bjorkblom, E. Rannikko, . . . E. T. Coffey. 2011. Phosphorylation of scg10/stathmin-2 determines multipolar stage exit and neuronal migration rate. Nat. Neurosci. **14:** 305–313. doi: 10.1038/nn.2755

斑馬魚 Stathmin 家族基因在胚發育時期之基因表現分析

史德芬[1,2#]、朱湘翎[1#]、李士傑[1,2,3,4,5*]

1. 國立臺灣大學動物學研究所，台北市羅斯福路四段一號，10617，臺灣，中華民國。
2. 國立臺灣大學生命科學系，台北市羅斯福路四段一號，10617，臺灣，中華民國。
3. 國立臺灣大學 生物技術研究中心，台北市羅斯福路四段一號，10617，臺灣，中華民國。
4. 國立臺灣大學發育生物學與再生醫學研究中心，台北市羅斯福路四段一號，10617，臺灣，中華民國。
5. 國立臺灣大學系統生物學研究中心，台北市羅斯福路四段一號，10617，臺灣，中華民國。

* 通訊作者。*Fax: 886-1-2-33662457; Tel.: 886-1-2-33665902; Email: jefflee@ntu.edu.tw*

此二作者在本論文有相同貢獻

(收稿日期：2014 年 02 月 07 日；接受日期：2014 年 04 月 04 日)

摘要：Stathmin家族基因因其細胞微管去組裝之功能而可整合不同細胞內訊息傳遞之路徑，然而我們對其在胚胎發育過程中所扮演之角色卻不甚明瞭，因此我們由斑馬魚中選殖出包括*stathmin 1b* (*stmn1b*)，*stathmin-like 2a* (*stmn2a*)，*stathmin-like 3* (*stmn3*)及*stathmin-like 4* (*stmn4*)等四種不同stathmin基因並分析其特性。此四種stathmin基因均帶有與哺乳動物相似且高度保守的類stathmin及可被磷酸化之區域。利用反轉錄聚合酶鏈式反應(RT-PCR)和全固定原位雜合反應分析(whole-mount *in situ* hybridization analysis，WISH)我們發現此四種斑馬魚*stathmins*主要表現在中樞神經系統，但其表現彼此間有時間及空間上之歧異，這也顯示了這些stathmin在斑馬魚發育過程中之神經發育可能扮演某些角色。在以嗎啉基寡核苷酸(morpholino oligonucleotide, MO)弱化stahmin基因之斑馬魚胚中我們觀察到下列表徵：頭部變小，腦室偏大，腦水腫及中後腦間隔變窄。同時我們亦以*islet1* 基因WISH的方法觀察神經之發育，也發現到*islet1*之表現在*stmn2a* MO處理之胚中明顯降低。這些缺陷無法在非對應性的*stmn2a* MO注射的胚中發現，更重要的其缺陷可為同時與*stmn2a* MO注射之*stmn2a* mRNA所救回。總之這些結果證實了*stmn2a*在斑馬魚腦部之發育扮演關鍵之角色。

關鍵詞：胚胎發育、基因表現、stathmin、斑馬魚。

SUPPLEMENTARY DATA

Table S1. Primer pairs used in this study

Gene	Accession no.	Sequence	Amplicon (bp)
Primer pairs			
stmn1b	CK352858*	Fw: 5'-GGATCCATGGCGTCCTCTGGAG-3' Rv: 5'- GGATCCCACGGAAAACTGGCCA-3'	551
stmn2a	CN510260*	Fw: 5'- CATGGCCAAAACAGCTATCG-3' Rv: 5'-GGCATGAAAAGGAGGAGGAG-3'	568
stmn3	GENSCAN00000023522+	Fw: 5'-ATGGACAGCACACTATCAGCATAC-3' Rv:5'-TTAACCAGAAAGATCAGTGTTAAGC-3'	546
stmn4	CN325025*	Fw: 5'- CATGACCTTGGCAGCATATC-3' Rv: 5'- GAAGTGCTCGCTCC TCTACC-3'.	583
ef1α	NM_131263	Fw: 5'-CAAGGAAGTCAGCGCA TACA-3' Rv: 5'-TGATGACCTGAG CGTTGAAG-3'	542
Stmn2a for mRNA	CN510260*	Fw: 5'-CATGcCgAAAAcAGgTATgG-3'# Rv: 5'-GGCATGAAAGGAGGAGGAG-3'	568

Underlined nucleotides indicate BamHI cutting sites hanging on the 5' end of the *stmn1b* primers.
* Predicted expressed sequence tag sequence by *in silica* cloning.
+ Predicted transcript sequence from ENSDARG00000038465 (Ensembl).

Table S2. Identity and similarity analyses of zebrafish stathmins

			Amino acid identity and similarity (%)*									
Gene name	**Length**	**Origin**	**1a_ZF**	**1b**	**1b_ZF**	**2a**	**2b_ZF**	**3**	**3_N**	**4**	**4_ZF**	**4l_ZF**
Stmn1a_ZF	148	NP_001035465	-	82/89	82/90	59/76	58/77	53/68	53/68	66/77	66/77	62/77
Stmn1b	149	Cloned		-	99/99	57/76	56/78	54/69	54/69	63/75	63/75	60/76
Stmn1b_ZF	149	NP_001017850			-	57/77	56/78	54/69	54/69	63/76	63/76	60/76
Stmn2a	180	Cloned				-	84/93	56/70	56/70	57/76	57/76	58/76
Stmn2b_ZF	180	NP_001019393					-	58/75	58/75	58/76	58/76	59/78
Stmn3	181	Cloned						-	100/100	52/69	52/69	50/69
Stmn3_N	181	XP_001339376							-	52/69	52/69	50/69
Stmn4	188	Cloned								-	99/99	74/84
Stmn4_ZF	188	NP_998566									-	74/84
Stmn4l_ZF	188	NP_001002563										-

*percent amino acid identity/percent amino acid similarity

Length of each stathmin is shown in number of amino acids.

ZF: Sequences annotated by ZFIN (http://www.zfin.org). N: Sequence annotated by NCBI (http://www.ncbi.nlm.nih.gov/).

Table S3. Identity and similarity analyses of stathmin family orthologs

	Amino acid identity and similarity (%)*											
	STMN1			STMN2			STMN3			STMN4		
	Human	Mouse	Frog	Human	Mouse	Frog	Human	Mouse	Frog	Human	Mouse	Frog
	(149)[a]	(149)	(145)	(179)	(178)	(178)	(180)	(180)	(180)	(216)	(189)	(185)
Stmn1a_ZF (148)	77/84	76/84	70/81	64/77	64/77	60/75	63/78	62/79	56/76	66/79	66/79	64/77
Stmn1b (149)	73/87	72/87	72/84	59/75	59/75	56/73	56/71	56/72	53/72	63/77	63/77	61/76
Stmn1b_ZF (149)	73/88	72/88	76/85	59/75	59/75	56/74	57/72	56/73	53/73	63/78	63/78	61/76
Stmn2a (180)	61/76	61/76	56/74	76/90	76/90	72/87	65/81	64/82	60/79	60/75	60/75	58/75
Stmn2b_ZF (180)	59/76	59/76	56/74	74/89	74/89	71/86	65/81	64/82	61/81	60/74	60/74	59/74
Stmn3 (181)	56/68	56/68	54/66	62/76	62/76	61/75	67/83	67/83	67/82	52/68	52/68	51/70
Stmn3_N (181)	56/68	56/68	54/66	62/76	62/76	61/75	67/83	67/83	67/82	52/68	52/68	51/70
Stmn4 (188)	68/79	67/79	66/79	62/77	62/77	56/74	57/75	57/75	55/74	81/88	81/88	76/84
Stmn4_ZF (188)	68/79	67/79	66/79	62/77	62/77	56/74	57/76	58/76	56/75	81/89	81/89	77/85
Stmn4l_ZF (188)	65/79	64/79	61/74	61/78	61/78	55/74	54/74	55/75	53/76	76/86	76/86	73/83

*percent amino acid identity/percent amino acid similarity

Length of each stathmin is shown in parenthesis.

Human: *Homo sapiens*; Mouse: *Mus musculus*; Frog: *Xenopus laevis*.

ZF: Sequences annotated by ZFIN (http://www.zfin.org). N: Sequence annotated by NCBI (http://www.ncbi.nlm.nih.gov/).

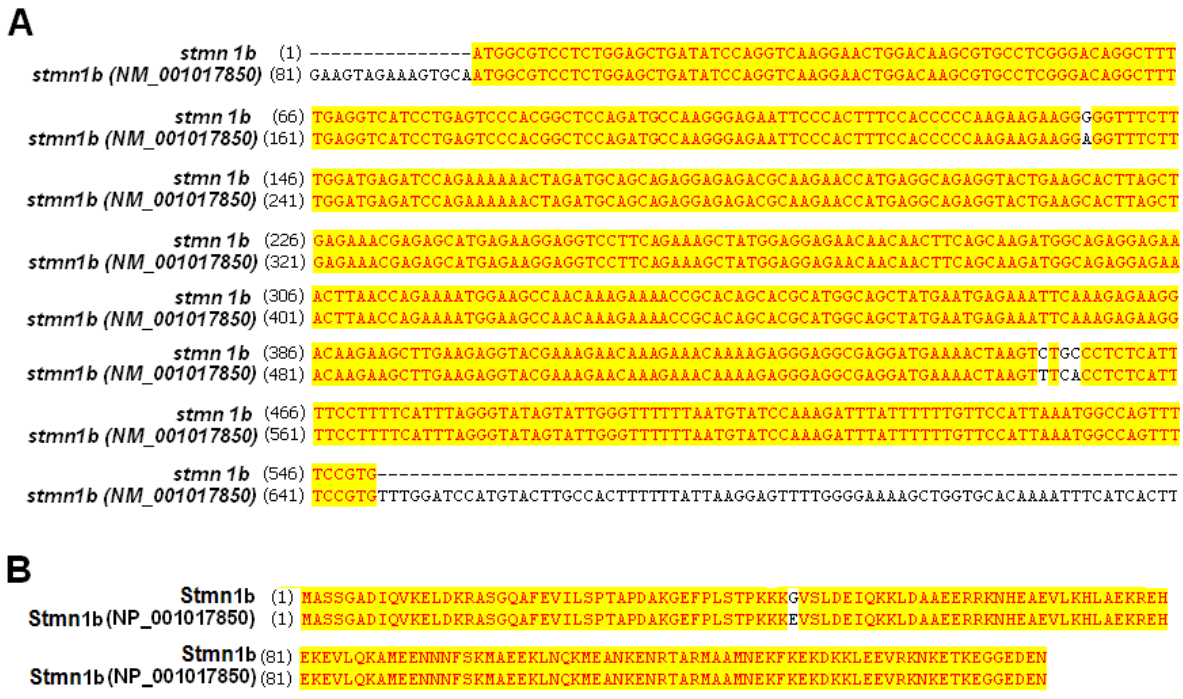

Fig. S1. Sequence alignment of stathmin 1b. A: Nucleotide sequences. B: Amino acid sequences.

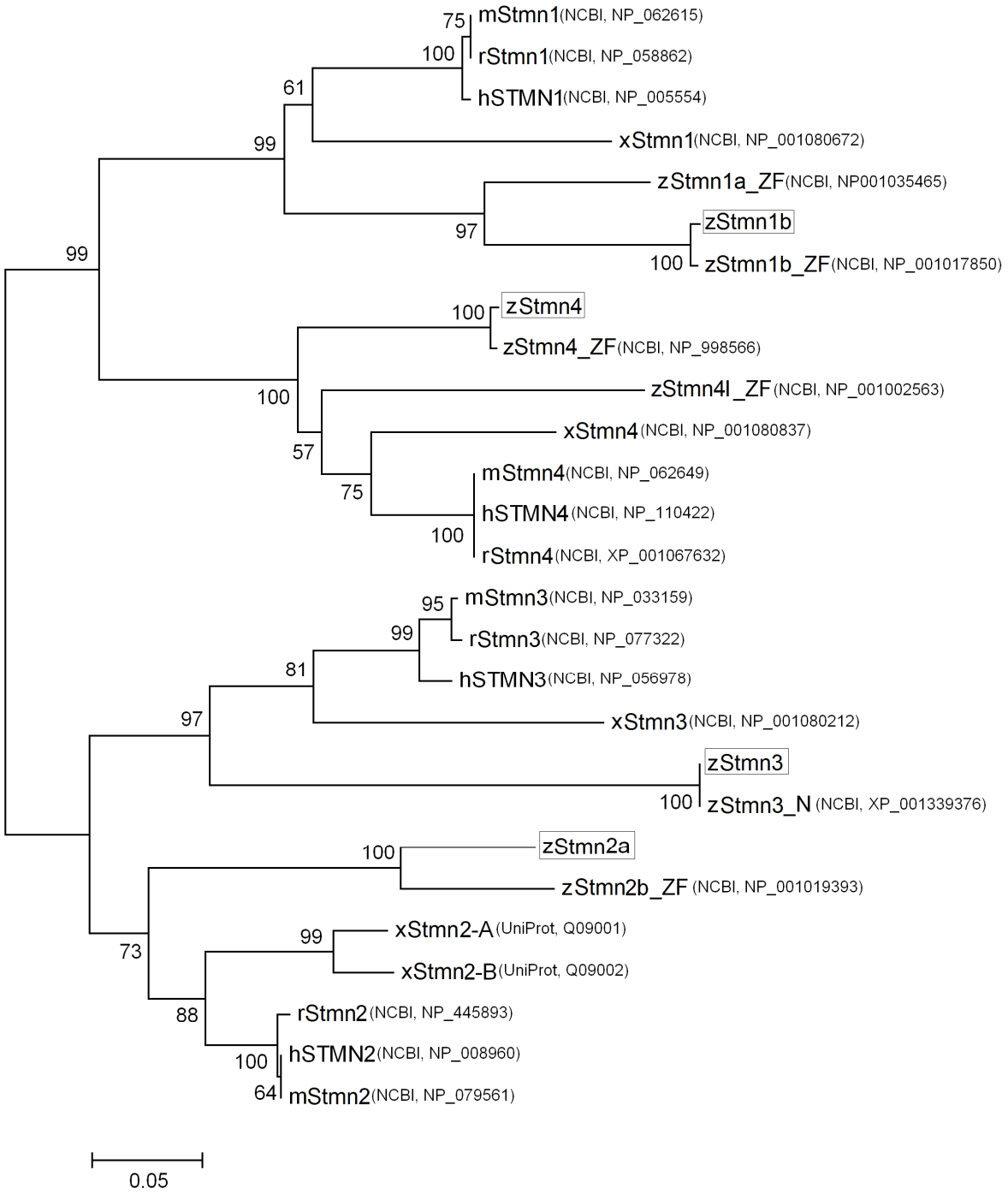

Fig. S2. Phylogenetic analysis of stathmin orthologs among vertebrates. The phylogenetic tree was constructed based on amino acid sequence alignments performed by ClustalW of MEGA4. Bootstrap values were calculated from 1000 replications using the Neighbor-joining method, and indicated at the branches. The suffixes _ZF and _N represent sequences annotated by the ZFIN and NCBI, respectively. The boxed proteins are deduced zebrafish stathmins identified in this study. h, *Homo sapiens*; m, *Mus musculus*; r, *Rattus novegicus*; x, *Xenopus laevis*; z, *Danio rerio.*

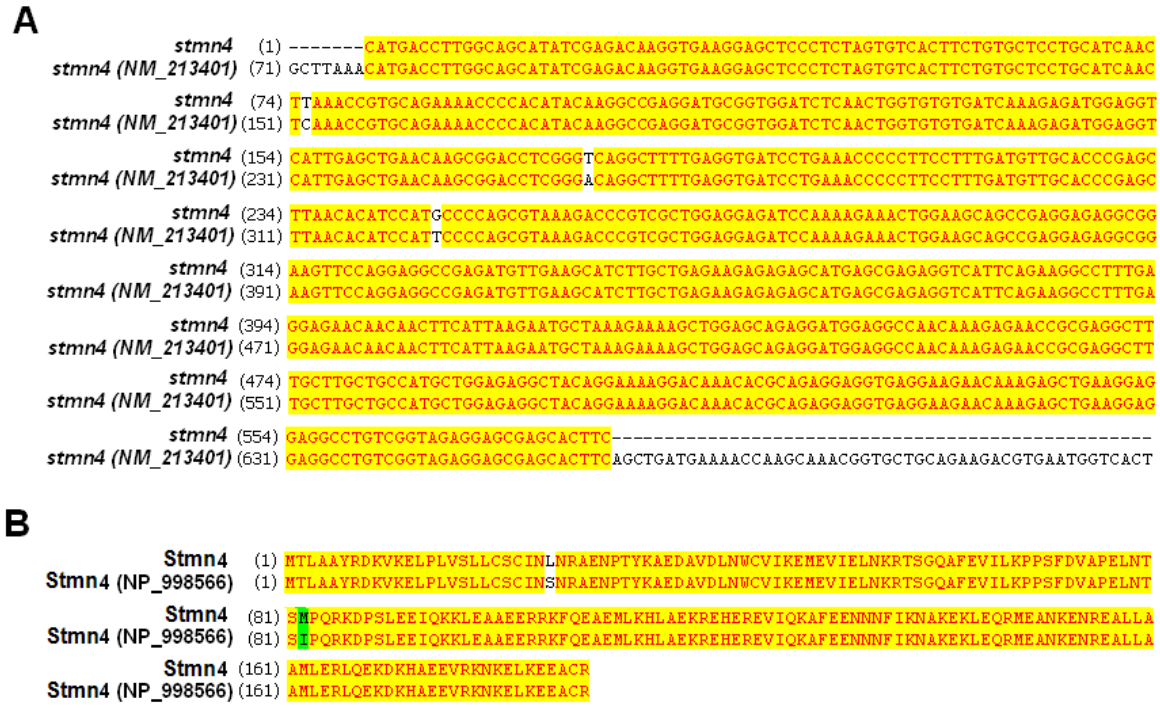

Fig. S3. Sequence alignment of stathmin 4 (A) nucleotide sequences (B) amino acid sequences

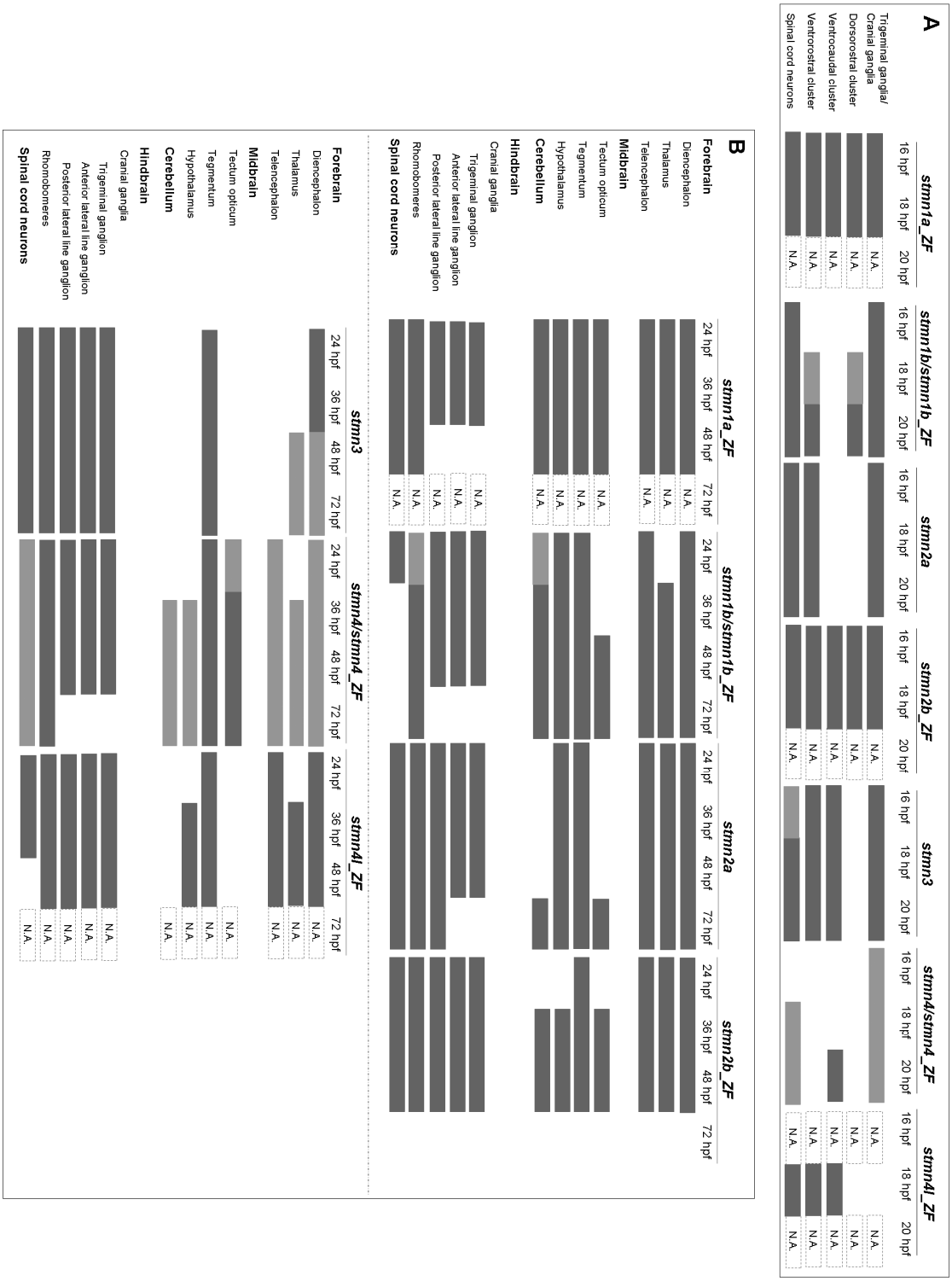

Fig. S4. Summary of the spatial expressions of stathmin family genes in the central nervous system. *stmn1b*, *stmn2a*, *stmn3*, and *stmn4* denote in situ hybridization results shown in Figs. 4 and 5; *stmn1a_ZF*, *stmn1b_ZF*, *stmn2ab_ZF*, *stmn4_ZF*, and *stmn4l_ZF* display expression patterns available on ZFIN (http://www.zfin.org). Expression patterns of zebrafish stathmin family genes at segmentation (A) and early larva stages (B). Black and grey bars denote strong and weak expression in the region for the respective gene, respectively. N.A.: expression patterns not available on ZFIN.